附件1-1 论文1 本项目成员关伟鹏、陈昕、黄谋潇、刘梓璇为论文作者

IEEE Photonics Journal
An IEEE Photonics Society Publication

Open Access

High-Speed Robust Dynamic Positioning and Tracking Method Based on Visual Visible Light Communication Using Optical Flow Detection and Bayesian Forecast

Volume 10, Number 4, August 2018

Weipeng Guan
Xin Chen
Mouxiao Huang
Zixuan Liu
Yuxiang Wu
Yingcong Chen

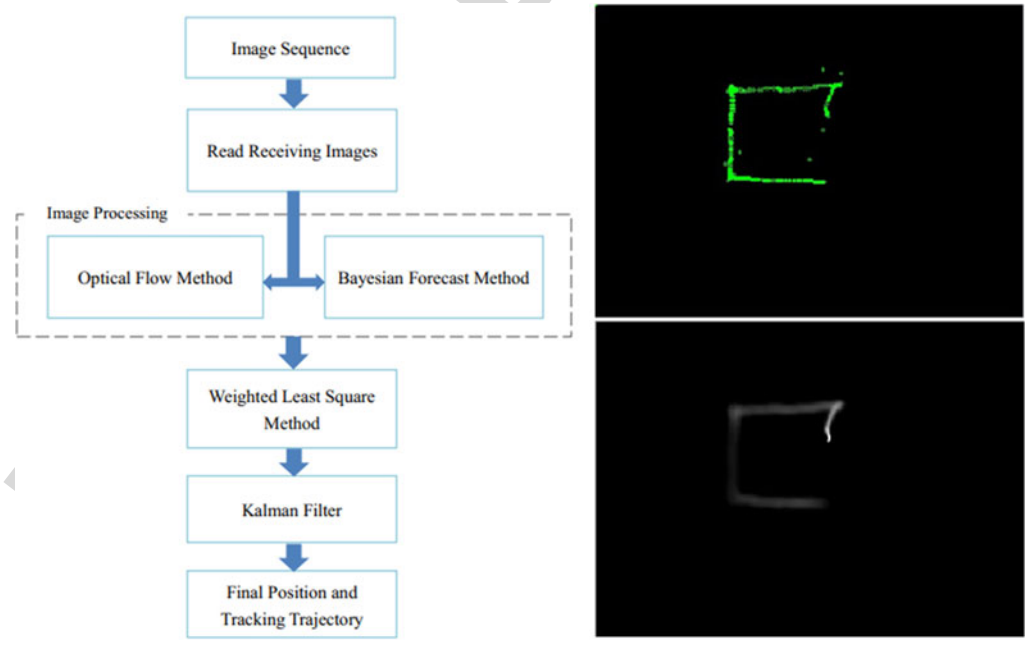

DOI: 10.1109/JPHOT.2018.2841979
1943-0655 © 2018 IEEE

High-Speed Robust Dynamic Positioning and Tracking Method Based on Visual Visible Light Communication Using Optical Flow Detection and Bayesian Forecast

Weipeng Guan,[1] **Xin Chen**,[1] **Mouxiao Huang**,[1] **Zixuan Liu**,[1] **Yuxiang Wu**,[1] **and Yingcong Chen**[2]

[1]School of Automation Science and Engineering, South China University of Technology, Guangzhou 510640, China
[2]Foshan Nanhai Guangdong Technology University CNC Equipment Cooperative Innovation Institute, Foshan 528000, China

DOI:10.1109/JPHOT.2018.2841979

Manuscript received May 7, 2018; accepted May 26, 2018. This work was supported in part by the National Undergraduate Innovative and Entrepreneurial Training Program under Grants 201510561003, 201610561065, 201610561068, 201710561006, 201710561054, 201710561057, 201710561058, 201710561199, and 201710561202; in part by the Special Funds for the Cultivation of Guangdong College Students' Scientific and Technological Innovation ("Climbing Program" Special Funds) under Grants pdjh2017b0040 and pdjha0028; and in part by the Guangdong science and technology project under Grant 2017B010114001. Corresponding authors: Weipeng Guan and Yingcong Chen (e-mail: augwpscut@mail.scut.edu.cn; cyc_scut@163.com).

Abstract: There are three critical elements in visible light positioning (VLP) system: Positioning accuracy, real-time ability, and robustness. However, most of the existing VLP studies only focus on the positioning accuracy and only a few studies consider the real-time ability at the same time. While the robustness is usually ignored in the field of VLP, which has a great impact on positioning performance or even leads to the failure of positioning. Therefore, we propose a novel VLP algorithm based on image sensor (as positioning terminal), exploiting optical flow detection and Bayesian forecast. The proposed optical flow method is used for real-time detection, and solves the problem of blur effect caused by the fast relative movement between the LED and positioning terminal, which would result in location failure in the traditional VLP system with pixel intensity detection. While the proposed Bayesian forecast algorithm is used for forecasting the possible location of the LED in the next frame image according to the previous frames as empirical data, which drastically solve the problem of shielded effect caused by the light link between the LED and the positioning terminal is shielded or broken. Finally, the detection location information and the forecast location information are fused by the Kalman filtering. Experimental results show that the positioning accuracy of the proposed algorithm is 0.86 cm, which realizes high positioning accuracy. The computational time of the algorithm process is about 0.162 s, and the proposed algorithm can support indoor positioning for terminal moving at a speed of up to 48 km/h. Both data demonstrate that the proposed algorithm has good real-time performance. Meanwhile, the proposed algorithm has strong robustness, which can handle the blur effect and the shielded effect in the traditional VLP system based on image sensor.

Index Terms: Visible light positioning (VLP), real-time positioning and tracking, image sensor (IS), optical flow, Bayesian forecast, robustness.

1. Introduction

With the emergence of various large structure, such as shopping malls, transit interchanges, hospitals and so on, the activity place becomes more and more complex. Therefore, the demand for indoor position is strongly increasing, and the requirement is becoming higher to meet the changeable need at the same time, which includes positioning accuracy, real-time ability and robustness. In recent years, there have been many indoor positioning techniques put forward to solve this problem such as wireless local area network (WLAN), Ultra Wideband (UWB), Bluetooth, ZigBee and Radio-frequency Identification (RFID), and so on. However, with the inherent flaws of themselves, some can't perform well in positioning accuracy, some are sensitive to electromagnetic interference leading to poor robustness, and others are not suitable for large-scale application as they require additional expensive devices. All of these traditional techniques are not fully up to expectation.

Different from the traditional positioning techniques mentioned above, visible light positioning (VLP) is applicable for indoor positioning owing to its advantages of illumination and relative high positioning accuracy. The future looks bright for VLP in the position field. Indoor positioning system based on VLP can be divided into two modes: the Photodiode-based (PD-based) positioning, and the image-sensor-based (IS-based) positioning [1]. To date, positioning based on PD has been deeply explored. In our prior works [2]–[7], we have completed a series of research project with VLP base on PD. According to these studies, it could be found that, as the PD is sensitive to the direction of the light beam, it greatly limits the mobility of the positioning terminal. Another drawback of PD-based positioning is that the positioning result depends on the angular measurements, the measuring of received signal strength, varying intensities of light, and the solving of quadratic equations for position estimation, leading to a large percentage of error. Also, it requires high-precision devices when it exploits time of arrival (TOA) or time difference of arrival (TDOA), and phase of arrival (POA) or phase difference of arrival (PDOA) to estimate the position of terminal. Therefore, using IS as the receiver of positioning terminal is a promising alternative. What's more, the IS-based VLP is immune to reflected light, while the PD-based VLP realizes positioning through the intensity of receiving light obtained from the direct and reflective channel [6]. Meanwhile, the image sensor in combination with commercial mobile phone, can be used in not only experimental condition but also without peripheral in practice. Last but not the least, hardly did the studies based on PD-based VLP explore the scope of dynamic positioning and tracking, which confined the application to static fixed-point positioning or low-speed motion positioning [8]. Although, there is few studies based on IS-based VLP take the real-time ability into consideration too, for the weakness of PD-based positioning mentioned above, the performance of image sensor is better than PD is the field of VLP [9], [10].

As for IS-based VLP, there are also a number of studies. In general, though the performance of image sensor is better than the PD in the field of VLP, these studies do not deliver satisfactory performance in terms of positioning accuracy, real-time ability and robustness, which are the three important factors in indoor positioning system. And the limitations of the existing studies are analyzed as follows: First of all, there is still much room for improvement in regard to positioning accuracy. In [11], receiving visible light information by photodiode and receiving visual information by the camera, and the 3-D positioning error is at the level of decimeter. In [12], a single LED positioning system based on circle projection using single LED with a marginal marker point is proposed and demonstrated, whose positioning accuracy is 25.12 cm. In [13], the positioning error can be minimized within 10 centimeters and it also has the benefits of device simplicity. In [14], the author proposed an algorithm using three LEDs and even realize a high positioning accuracy of mm-level in the computer simulation. However, those work only focus on the static positioning and overlooked the real-time ability of the VLP system. In practice, the advantage of high positioning accuracy can't make up the disadvantage of low computational rate (poor real-time ability). As for the real-time, few studies maintain a balance between real-time and positioning accuracy. In [15], MiniMax filter is used for terminal trajectory estimation at average velocity of 1 m/s (3.6 km/h), but the velocity still can't meet the requirement of real-time, which only adapt to the positioning terminal

with low speed motion. Beside it was just theoretical simulation in the MATLAB simulator. In [16], the author take the real-time ability into account, it supports indoor positioning for terminal moving at a speed of up to 18 km/h, and achieves the positioning accuracy of 7.5 cm. This work create a new era in VLP, which take both positioning accuracy and real-time into consideration. However, reference [16] does not take into account the fact that the image of LED will blur and the detection of LED-ID will fail when the terminal moves in such speed. This work ignores the robustness which is usually ignored in the field of VLP. On the one hand, there is a high probability of great error, since this work does not discuss the motion blur. The IS-based positioning method in [16] is based on pixel intensity detection, so when the positioning terminal moves too quickly, the LED image would suffer from blur effect, which causes difficulty to find the center of LED and recognize the ID of LED through the pixel intensity, and the positioning would fail. Therefore, when there has the fast relative movement between the LED and positioning terminal, the proposed VLP system in [16] would fail to locate. The blur effect is the main restrictions of the real-time ability and robustness in VLP. On the other hand, apart from the motion blur, notably, all of the study in VLP didn't take into account the general situation where the transmitter (i.e., LED) is shielded or broken. When the light links between the LEDs and the positioning terminal is blocked, even just one of the light links, the positioning would fail. Because all of the positioning algorithm in VLP are based on 2 or 3 and even more LEDs, when the number of LEDs in the view of image sensor decreases, the positioning would fail. The shielded effect is the fatal shortcoming in the VLC or VLP, which also leads to poor robustness and no one has yet solved it.

Motivated by the pressing problems, in this paper, we propose high-speed robust dynamic positioning and tracking algorithm based on image sensor using optical flow detection and Bayesian forecast. The proposed optical flow algorithm is used for solving the problem of blur effect caused by the fast relative movement between the LED and positioning terminal, and decreases the computational cost to realize the real-time ability. While the proposed Bayesian forecast algorithm is used for forecasting the possible location of the LED in the next frame image according to the previous frames as empirical data, which drastically sorts out the problem of shielded effect caused by the light link between the LED and the positioning terminal is shielded or broken. Finally, the detection location information from optical flow and the forecast location information from Bayesian are fused by Weighted Least Square Method (WLS). Then the synthetic information is considered as the input of the Kalman filtering to output the trajectory of the positioning terminal. The remainder of this paper is organized as follows. Section 2 provides a detail derivation of the proposed positioning and tracking algorithm. The experimental setup and analysis are presented in Section 3. Finally, in Section 4, we summarize our work.

2. Theory

The IS-based VLP utilizes the rolling shutter mechanism of the Complementary Metal Oxide Semiconductor (CMOS) image sensor, whose working principle is shown in Fig. 1(a), to realize LED-ID recognition. The exposure and data readout are performed row by row, the data of one row read out immediately when the exposure of this row is finished. This is known as the rolling shutter mechanism. By the rolling shutter mechanism of CMOS sensor, turning on and off the LED light during a period of exposure would result in bright and dark stripes on the image captured by CMOS sensor [9], [10]. In the IS-based VLP, there are several LEDs in an image at the same time. Fig. 1(b) shows the process of the LED-ID modulation and recognition, in our previous research [9], [10], we have describe the detailed processing of LED-ID modulation and demodulation. For the readers that are interested in the LED-ID modulation and recognition, please refer to our previous reports.

The proposed positioning and tracking algorithm considers three main problems in VLP: (1) The computational cost of the existing VLP methods is so huge that it is hard to ensure the real-time ability of the algorithm. (2) Some frames suffer from blur effect when the positioning terminal moves at a high speed, which causes failure of LED detection and eventually result in the failure of positioning. (3) There are usually some obstacles in the way of the propagation between the LED and positioning terminal, which is the shield effect. The last two problems both relate to the

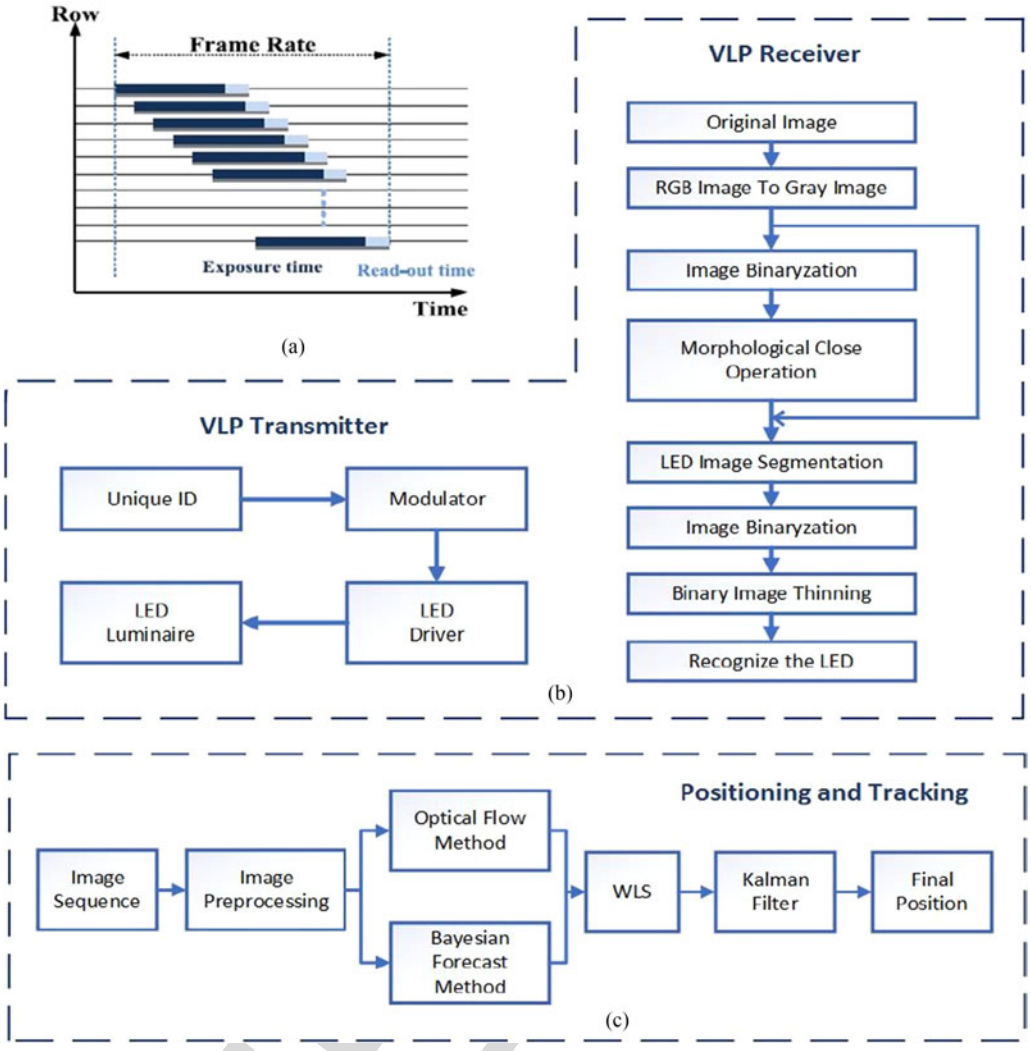

Fig. 1. (a) the rolling shutter mechanism of the CMOS; (b) the processing of LED-ID modulation and recognition; (c) The architecture of positioning and tracking algorithm using optical flow detection and Bayesian forecast.

poor robustness in the traditional VLP. In essence, dynamic positioning and tracking is analyzing the captured image sequences and estimating the position with strategy. It's worth to mention that the video target tracking method, which can obtain the valid data of the image to decrease the computational cost as well as improve the positioning accuracy. After detecting the LED in the first frame, the proposed positioning and tracking algorithm can automatically estimate the LED position in the following frames with some strategy, which significantly improves the computation efficiency. Hence, it is especially suitable for practical scene. With the method of optical flow and Bayesian forecast, our proposed method exploits video target tracking, which contains three parts, detection, prediction and tracking. The LED is detected by optical flow and solve the problem of blur effect from which the tradition detecting method of pixel intensity suffers. At the same time, predict the probability position of target LED via Bayesian forecast to ensure the positioning when the LED is shielded. Meanwhile, Bayesian forecast makes the algorithm better to position on IS which is as same as the positioning terminal's in advance, that is to say, the computational speed of this algorithm is also improved. Last but not the least, the result of optical flow detection and Bayesian

forecast are partially combined by WLS, and the fusion location information of the detection and forecast are used as the input observation value of Kalman filtering to estimate the final position of the positioning terminal. The whole algorithm architecture is illustrated in Fig. 1(c). In the following parts, we will formulate the problem mathematically and illustrate the algorithm theoretically in detailed.

2.1 Detection

In the traditional positioning based on IS, LEDs (or LED-ID) are detected according to pixel intensity. In this way, it is easy to detect the LEDs by setting a threshold value. However, the blur effect would occur in the LED images when the LED and the IS have a high speed of relative motion, making it difficult to detect the LEDs as well as the LED-ID through merely using image recognition method. Without detecting the LED and LED-ID correctly, it causes the failure of positioning. To address the issues mentioned above, the proposed optical flow algorithm is used as the motion feature of LED for detection. The basic concept of optical flow method is to get the motion parameters of moving positioning terminal, which is denoted by optical flow vector.

In order to calculate the optical flow, an assumption is made based on the optical properties of the object's movement [17]: the intensity structures found in the image, on a local level, remain approximately constant over time, at least during small intervals of time. It also valid within the short time between two frames. The brightness of a particular point in the pattern is constant, when the pattern moves in Δt and Δt to become zero. Just as the following:

$$I\left(x+\Delta x, y+\Delta y, t+\Delta t\right) = I\left(x, y, t\right) \tag{1}$$

where $I(x, y, t)$ represents the image brightness at the point (x, y) in the image plane at time t. Using chain rule to differentiate Equation (1), as follows:

$$I_x u + I_y v + I_t = 0 \tag{2}$$

where $u = \frac{dx}{dt}$, $v = \frac{dy}{dt}$, $I_x = \frac{\partial I}{\partial x}$, $I_y = \frac{\partial I}{\partial y}$, $I_t = \frac{\partial I}{\partial t}$. The local smoothness constraint assumption is that the optical flow is kept constant in a small local area Ω [18]. The overdetermined equation can be computed from Equation (2), as follows:

$$I_X\left(X_i\right) u + I_y\left(X_i\right) v + I_t\left(X_i\right) = 0 \quad \left(X_i \in \Omega,\ (i = 0, 1, \ldots . n-1)\right) \tag{3}$$

The optical flow estimation error is defined as:

$$E = \sum_{x,y\in\Omega} W^2\left(X\right)\left(I_x u + I_y v + I_t\right)^2 \tag{4}$$

where Ω is a small local area which has $\mathrm{n} = \mathrm{m} \times \mathrm{m}$ pixels, W(X) is a weighting function of each pixel in the area Ω which generally follows the Gaussian distribution. Minimizing E by using the least square method as follows:

$$A^T W^2 A\, V = A^T W^2 b \tag{5}$$

where $\mathrm{A} = [\nabla I(X_1), \ldots, \nabla I(X_n)]$, $\mathrm{b} = -(I_t(X_1), \ldots, I_t(X_n))^T$ and $\mathrm{W} = \mathrm{diag}(\mathrm{W}(X_1, \ldots, X_n))$. The solution of Equation (5) is

$$V = \left[A^T W^2 A\right]^{-1} A^T W^2 b \tag{6}$$

In a temporal consecutive sequence of 2-D images, the set of pixels which belong to LED is defined as:

$$\begin{cases} \left(x_i^t, y_i^t\right) \in L^t & for \quad V_{\left(x_i^t, y_i^t\right)} > T \\ \left(x_i^t, y_i^t\right) \notin L^t & for \quad V_{\left(x_i^t, y_i^t\right)} < T \end{cases} \tag{7}$$

where L^t represents the set of pixels which belong to LED at time t, the subscript i stands for the ith pixel in the image, T is a metric from $R^2 \rightarrow R$. The moving LEDs detected by using optical flow

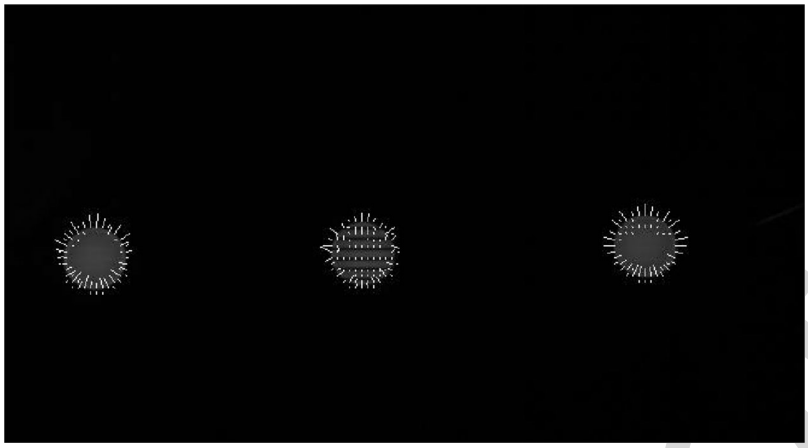

Fig. 2. The LED pixel detected by the optical flow.

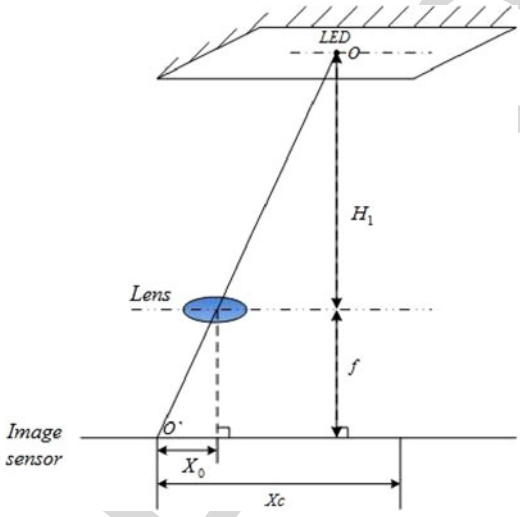

Fig. 3. Geometrical relationship between LED and image sensor.

method are illustrated in Fig. 2. Due to the area of background is much larger than that of LED, the coordinate of the LED s(t) (x^t, y^t) in the image, called the pixel coordinate of LED, is assumed to be the centroid of L^t.

In order to access the IS's world's coordinate $z_l(t)$, the proposed algorithm makes use of the geometric relations in positioning system showed in Fig. 3 and various coordinates systems showed in Fig. 4. With the focus of lens f, the size of each pixel on IS dx and dy, the ordinate of world coordinate of the lth LED D_l (x_l, y_l, z_l), the height H_l known. The process of computing z_l(t) (x_l^t, y_l^t, z_l^t) is explained as follows: Firstly, the pixel coordinate (x_0, y_0) of the centroid of the image can be calculated as follows:

$$\begin{bmatrix} x_0 \\ y_0 \\ 1 \end{bmatrix} = \begin{bmatrix} \frac{1}{dx} & 0 & x^t \\ 0 & \frac{1}{dy} & y^t \\ 0 & 0 & 1 \end{bmatrix} \begin{bmatrix} x_i^t \\ y_i^t \\ 1 \end{bmatrix} \tag{8}$$

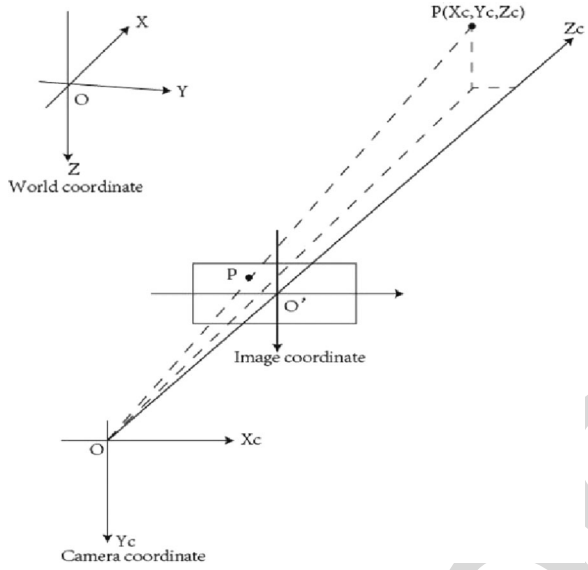

Fig. 4. Word coordinate system, Camera coordinate system and Image coordinate system.

After calculating the coordinate of the centroid of the image in the image coordinates (X_0, Y_0), the horizontal coordinate of camera in the camera coordinate X_C is computed as following equation:

$$\frac{X_0}{X_C} = \frac{f}{f + H_I} \tag{9}$$

Y_C can be calculated in the same way. Then (X_C, Y_C) can be transformed to (x_I^t, y_I^t) through a matrix as follows:

$$\begin{bmatrix} X_C \\ Y_C \\ 1 \end{bmatrix} = \begin{bmatrix} r_{00} & r_{01} & r_{02} \\ r_{10} & r_{11} & r_{12} \\ r_{20} & r_{21} & r_{22} \end{bmatrix} \begin{bmatrix} x_I^t \\ y_I^t \\ 1 \end{bmatrix} + \begin{bmatrix} T_X \\ T_Y \\ T_Z \end{bmatrix} \tag{10}$$

where, (x_I^t, y_I^t) is denoted by $z_I(t)$ which can be computed from Equation (8)$\sim$(10). Define that:

$$z_I(t) = h\left(s(t), D_I\right) \tag{11}$$

where D_I represents the Ith coordinate of the LED in the world coordinates fixed and known, h is the mapping function.

2.2 Prediction

There has been an unsolved problem in VLP that when an obstacle gets in the way of optical propagation between the transmitter and receiver (i.e., IS), the positioning will fail. This is a fatal flaw of existing studies but most of them avoid mentioning it. To overcome this great difficulty, the proposed algorithm adopts Bayesian forecast. It can predict the probable position in the next frame according to the frames before, therefore, achieving positioning when the LED is shielded. The basic idea of the prediction is using a random sample with weight to denote the distribution of random variable. When analyzing time varying problems, the space state model is decomposed into measurement and state propagation model. Due to the temporal continuity of the sequence of 2-D images, the frame number is assumed to be the same as time t and the LED is detected as illustrated in Fig. 5. In this way, we can also discretize the problem by setting sample frame number $k = mT \in [t_0, t]$ for $k = 0, 1, \ldots K$. Without loss of generality, t_0 is defined as 0. Note that the missed

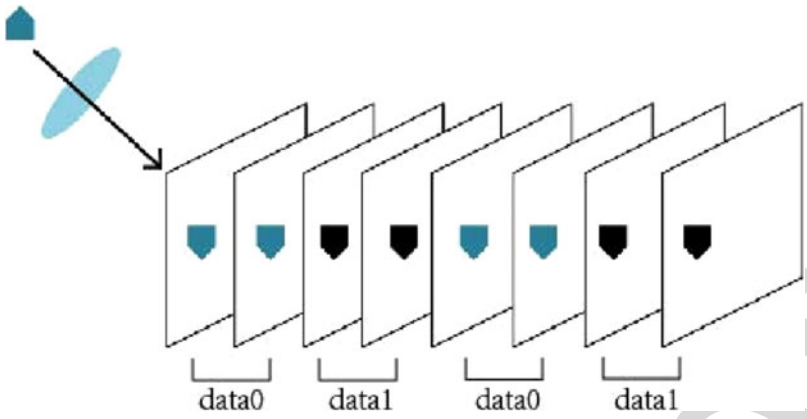

Fig. 5. Depicted sequence of camera images of a scene containing a blinking LED.

LED is taken in consideration. The variable $s(t)$ evolves according to Section 2.1, as follows:

$$s(t) = f\left(x^t, y^t\right) \tag{12}$$

where f is defined in Section 2.1, which represents the mapping between {x, y} and s. The lth LED at known and fixed location D_l projects onto the IS at position $z_l(t)$ from (11) at time t. The measurement of z is modeled as follows:

$$\tilde{z}_l(t) = h\left(s(t), D_l\right) + n_{z_l}(t) \tag{13}$$

where $n_{z_l}(t)$ represents the additive measurement noise. In the proposed algorithm, the symbol $\hat{s}$ represents the estimate of variable s. Given an initial value $s(0) \sim (0, 0)$. The estimate of $s(t)$ is:

$$\dot{\hat{s}}(t) = f\left(\hat{x}_i^t, \hat{y}_i^t\right) \tag{14}$$

Define $\xi s(t) = s(t) - \hat{s}(t)$ as the state error. The discrete-time equivalent error propagation model is:

$$\xi s(k) = A_{k-1}\, \xi s(k-1) + W_{k-1} \tag{15}$$

where $s(k)$ represents $s(mT)$ and W_{k-1} is the process noise which has the power spectrum density denoted by α_{k-1}. The state error covariance matrix Q_k evolves over $[t_0, t]$ according to Equation (16):

$$Q_k = A_{k-1} Q_{k-1} A_{k-1}^T + \alpha_{k-1} \tag{16}$$

where A_{k-1} is defined as state error transition matrix and process noise covariance α_{k-1} are discussed in [19]. When the estimate of the LED' s coordinate in the pixel coordinates at time-step {0, 1, . . . , K} is known, it is easy to compute both the predicted measurement position of the lth LED $\hat{z}_l(k)$ projected on IS by using the method introduced in Section 2.1 and its error covariance matrix $Z_l(k)$ can be calculated as follows:

$$\hat{z}_l(k) = h\left(s(k), D_l\right) \tag{17}$$

$$Z_l(k) = H_{l,k} Q_k H_{l,k}^T + U_{l,k} \tag{18}$$

where $H_{l,k}$ is the linearized measurement matrix and $U_{l,k} = cov(n_{z_l}(k))$ [20]. Then it is going to discuss how to deal with the problem that multiple probable LEDs are detected. Let $X_k \geq 0$ represent the number of detected probable LEDs in the predicted region $\Lambda_\sigma(k)$ at time k. Define the set of measurement at time-step k as:

$$Z(k) \triangleq \{z_m(k)\}_{m=1}^{X_k} \tag{19}$$

where z_m(k) denotes the location projected onto IS of the mth measurement hypothesis. It's worth mentioning that at most one measurement in Z(k) was generated by the LED while the others are false detections. Take none of the hypothesis generated by LED into account, the number of data association hypotheses at time k is $(X_k + 1)$. The situation that the LED is missed is denoted by $m = 0$. Herein, $m \in \{0, \ldots, X_k\}$. And define the set of the sum of measurements at time k as:

$$Z^k \triangleq \left\{ Z(\beta)_{\beta=1}^{k} \right\} \tag{20}$$

For a time window with K time steps, the number of joint data association hypotheses is:

$$E_k = \prod_{i=1}^{k} (X_i + 1) \tag{21}$$

where $\rho^{k,\beta}$ represents a list of joint data association hypotheses up to time step k, where $\beta \in \{1, \ldots, E_k\}$. Defining that:

$$\rho^{k,\beta} = \{m_1, m_2, \ldots, m_k\}. \tag{22}$$

When $\rho^{k,\beta} = \{\rho^{k-1,\lambda}, m_k\}$, $\rho^{k-1,\lambda}$ is assumed to be the parent hypothesis of $\rho^{k,\beta}$. Defining the set of LED's coordinates in the pixel coordinates as:

$$S^K = \{s(\beta)\}_{\beta=0}^{K} \tag{23}$$

Then the joint probability of an association hypothesis up to time step $k \in \{1, \ldots, K\}$ is defined in equation (24), as follows:

$$\mathrm{p}\left(\rho^{k,\beta} \middle| \ Z^k, \mathrm{S}^{k-1}\right) = \frac{1}{\mathrm{c}} p\left(Z(k) \middle| \rho^{k,\beta}, Z^{k-1}, \mathrm{S}^{k-1}\right) p\left(\rho^{k,\beta} \middle| Z^{k-1}, \mathrm{S}^{k-1}\right) \tag{24}$$

where the normalization factor $\mathrm{c} = \mathrm{p}(\mathrm{Z(k)}|Z^{k-1}, \ S^{k-1})$ is independent of the data association hypothesis $\rho^{k,\beta}$. Then the simplification of Equation (21) is computing by application of the general multiplication rule for conditional probability, as follows:

$$\mathrm{p}\left(\rho^{k,\beta} \middle| \ Z^k, \mathrm{S}^{k-1}\right) = \frac{1}{\mathrm{c}} p\left(Z(k) \middle| \rho^{k,\beta}, Z^{k-1}, \mathrm{S}^{k-1}\right) \mathrm{p}\left(\rho^{k,\beta}(\mathrm{k}) \middle| \rho^{k-1,\lambda}, Z^{k-1}, \mathrm{S}^{k-1}\right) \times \mathrm{p}\left(\rho^{k-1,\lambda} \middle| Z^{k-1}, \mathrm{S}^{k-2}\right) \tag{25}$$

We use the method of [21], so that Z^k and Z(k) only contain the measurement position information. On account of different sources they come from, the measurements in $Z(k)$ is independent. The first term on the right-hand of Equation (25) is equivalent to Equation (26), as follows:

$$p\left(Z(k) \middle| \rho^{k,\beta}, Z^{k-1}, \mathrm{S}^{k-1}\right) = \prod_{m=1}^{X_k} p\left(z_m(k) \middle| \rho^{k,\beta}, Z^{k-1}, \mathrm{S}^{k-1}\right) = \prod_{m=1}^{X_k} g_z(m) \tag{26}$$

It's assumed that measurements resulted from clutter are uniformly distributed in the predicted region and the noise follows Gaussian distribution so that the function $g_z(m)$ in (26) is:

$$g_z(m, m_k) \begin{cases} \frac{1}{M_k} & \text{for clutter} \\ & (m \neq m_k) \\ \mathcal{N}\left(z_i(k); \hat{z}^q(k), Q^q(k)\right) & \text{for the LED} \\ & (m = m_k) \end{cases} \tag{27}$$

where M_k is the size of the predicted region $\Lambda_\sigma(k)$ and function $N(z_m(k); \hat{z}^q(k), Q^q(k))$ evaluates at $z_m(k)$ with expectation $\hat{z}^q(k)$ and covariance $Q^q(k)$. Then the joint prior probability of the current position measurements is defined in Equation (28), as follows:

$$\mathrm{p}\left(Z(k) \middle| \rho^{k,\beta}, Z^{k-1}, \mathrm{S}^{k-1}\right) = \begin{cases} \frac{1}{M_k{}^{X_k}} & \text{if } \rho^{k,\beta}(k) = 0 \\ \frac{N(z_m(k);\, \hat{z}^q(k), Q^q(k))}{M_k{}^{X_{k-1}}} & \text{if } \rho^{k,\beta}(k) \neq 0 \end{cases} \tag{28}$$

$p(\rho^{k,\beta}(k)|\rho^{k-1,\lambda}, Z^{k-1}, S^{k-1})$ is computed through:

$$\mathrm{p}\left(\rho^{k,\beta}(k)\,|\rho^{k-1,\lambda}, Z^{k-1}, \mathrm{S}^{k-1}\right) = \begin{cases} (1-P_{ON})\,\eta_{xM_k}(X_k) & \text{if } \rho^{k,\beta}(k)=0 \\ \frac{1}{X_k} P_{ON}\,\eta_{xM_k}(X_k-1) & \text{if } \rho^{k,\beta}(k)\neq 0 \end{cases} \tag{29}$$

where P_{ON} is the probability of the LED is ON and the η_{M_k} is the posterior probability mass function of the number of false measurements due to clutter or noise. The parameter x represents the spatial density of clutter measurements. The term xM_k is the expected number of clutter measurements in the predicted region. The probability P_{ON} depends on the coding scheme and information content that each LED sends. Then the marginal likelihood that the mth measurement at time k originated from the LED is defined in Equation (30):

$$\mathcal{L}_{q,m}(\mathrm{k}) = \mathcal{N}\left(z_m(k); \hat{z}^q(k), Q^q(k)\right) P_{ON} \tag{30}$$

Therefore, Equation (31) can be computed, as follows:

$$\mathrm{p}\left(\rho^{k,\beta}(k)=i|Z^{k-1}, \rho^{k-1,\lambda}, \mathrm{S}^{k-1}\right) = \frac{\mathcal{L}_{q,m}(\mathrm{k})}{\sum_{j=0}^{X_k}\mathcal{L}_{q,j}(\mathrm{k})} \tag{31}$$

where $\rho^{k,\beta}(k)=m$ is the extension of joint hypothesis of $\rho^{k-1,\lambda}$. Only the marginalized probability is ought to be calculated. The best extension of $\rho^{k-1,\beta}$ is defined in Equation (32), as follows:

$$\rho^{k,\beta 1} = \left\{\rho^{k-1,\beta}, m_k\right\}, \quad \text{where} \quad m_k = \operatorname{argmax}\mathcal{L}_{\beta,m}(k) \tag{32}$$

So that the best predicted measurement position of the lth LED projected on IS $\hat{z}_l(k)$ could be computed. The proposed algorithm can find the list of best predicted measurements, which is considered as the estimated motion trajectory, by calculating $\hat{z}_l(k)$ incrementally.

2.3 Tracking

To realize real-time dynamic positioning and tracking, we need to screen constantly and process every frame, detect the LED and calculate the position of the positioning terminal in real time. It's of great calculation and poor real-time if we detect LED in every frame taken, reducing the tracking precision. Therefore, in order to track in real time as precisely as possible, this paper proposes a new method, which combines Sections 2.1 and 2.2 by using Kalman. We can get the measurement position information and predicted position information via optical flow and Bayesian forecast respectively. Then, take advantage of Kalman to combine this two information. The reason why we do that is to ensure the proposed algorithm can fit in different situations with high positioning accuracy. When the target (i.e., LED) is shielded, the optical flow is invalid, thus making the algorithm automatically improve the weight of predicted position information so that it can position and track normally. When there is no obstacle in the way of propagation between the transmitter and receiver, the position information of optical flow will be the main factor of the final result as the error of Bayesian forecast is larger than that of optical flow. It secures the algorithm can perform with strong robustness. The detailed computing tracking and positioning results is illustrated in Fig. 6.

The coordinate of LED in the pixel coordinates $s(k)$ is known after processing the image sequences. The Kalman model assumes the true state at time step k denoted by $Z_l^R(k)$ is evolved from the state at $(k-1)$ as:

$$Z_l^R(k) = B_k Z_l^R(k-1) + V_k \tag{33}$$

where B_k is the state transition model which is applied to the previous state $Z_l^R(k-1)$ and V_k is the process noise which is assumed to be drawn from a zero-mean multivariate normal distribution $\mathcal{N}$ with covariance Q_k. And the observation equation at time k is defined as follows:

$$y_i(k) = F_{ik} Z_l^R(k) + G_{ik}, \ (i=1,2) \tag{34}$$

where F_{ik} is the observation model which maps the true state space into the observed space and G_{ik} is the observation noise which is assumed to be zero mean Gaussian white noise with covariance

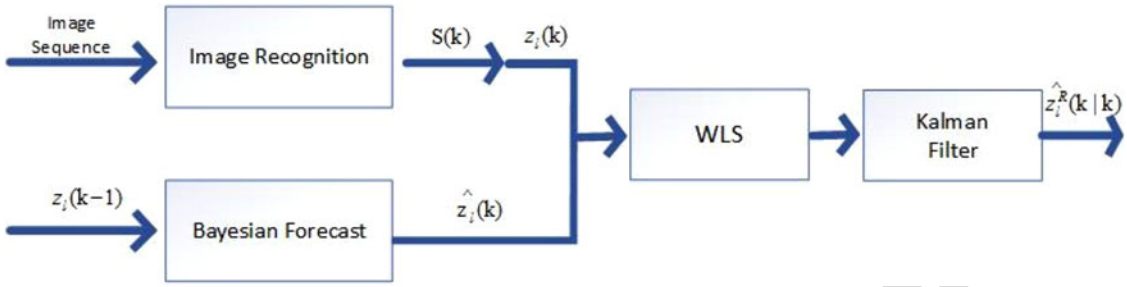

Fig. 6. Process of computing final result of the positioning terminal.

R_{ik}. In this paper, $y_1(k)$ denotes $z_l(k)$ and $y_2(k)$ denotes $\hat{z}_l(k)$. The Equation (34) is equivalent to Equation (35) by using WLS (Weighted Least Square Method):

$$y(k) = F_k Z_l^R(k) + G_k \tag{35}$$

Five basic equations are listed as follows:

$$\hat{Z}_l^R(k|k-1) = B_k \hat{Z}_l^R(k-1|k-1) \tag{36}$$

$$P(k|k-1) = B_k P(k-1|k-1) B_k^T + Q_k \tag{37}$$

$$\hat{Z}_l^R(k|k) = \hat{Z}_l^R(k|k-1) + K_k \left(y(k) - F_k \hat{Z}_l^R(k|k-1) \right) \tag{38}$$

$$K_k = P(k|k-1) F_k^T \left(R_k + F_k P(k|k-1) F_k^T \right)^{-1} \tag{39}$$

$$P(k|k) = (I - K_k F_k) P(k|k-1) \tag{40}$$

where $\hat{Z}_l^R(k|k-1)$ represents the posteriori state estimate at time step k given observations up to and including at time step k, $P(k|k)$ represents the posteriori error covariance matrix of the state estimate at time step k and K_k denotes optimal Kalman gain. The true state at time step k which is denoted by $Z_l^R(k)$ can be composed as shown in Equation (34) which can be explained by principle:

$$\hat{Z}_l^R(k|k) = \varepsilon \hat{Z}_l^R(k|k-1) + (1-\varepsilon)\ y(k) \tag{41}$$

where ε denote the weight ($\varepsilon < 1$) which can updates automatically. Note that $\hat{Z}_l^R(k-1)$ gets closer to the real position over time. With this method, we can realize tracking in real time more precisely by using optical flow method even if the LED is missed. Meanwhile, the robustness, running time and tracking speed of the tracking algorithm is greatly improved in the case that the LED is missed and motion blur. At the same time, the positioning area is enlarged besides LEDs through prediction method.

3. Experimental Setup and Result Analysis

3.1 Experimental Setup

The experimental platform is shown in Fig. 7, includes a constant voltage source, four LEDs, a smart car, an industry camera and a computer (Dell Inspiron 5557, Windows 10, 4G RAM, Intel(R) Core(TM) i5-6200 CPU @ 2.4GHz). Constant voltage source supplies power to LEDs. The LED emits the optical signal as a transmitter and the industry camera receives this signal as a positioning terminal. The smart car is a carrier for the industry camera, simulating mankind indoor movement. The computer processes the received image from the industry camera with the proposed positioning and tracking algorithm to detect the LEDs and position the camera in real time.

There are four LEDs located on the ceiling of the system configuration in an experimental platform with the size of 190 cm × 100 cm × 190 cm. The LEDs' coordinates (in cm) are (100,145,190),

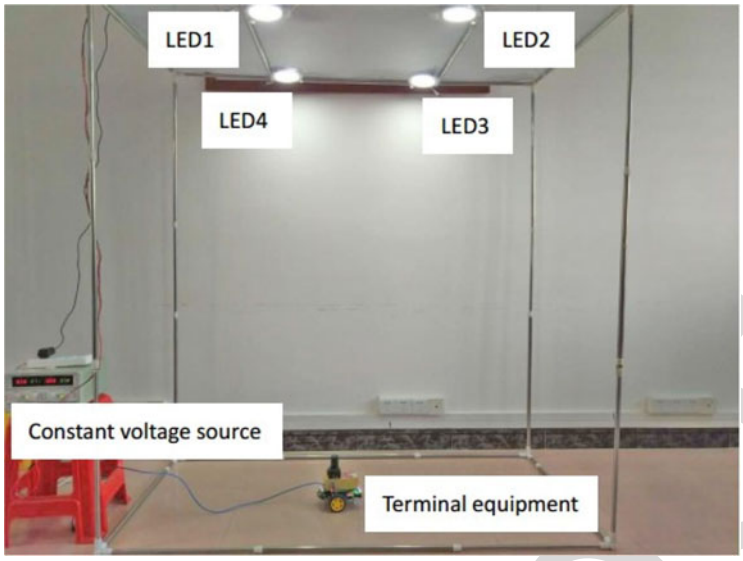

Fig. 7. Hardware of the proposed experiment configuration.

(0,145,190), (0, 45, 190) and (100, 45, 190), respectively. Specifications of the industry camera, experimental platform, LED, the smart car and circuit board are shown in Table 1.

The open source computer vision library (OpenCV3.2.0) is used to process receiving images with C++ language as the software system. The detailed algorithm procession of the proposed tracking and positioning algorithm using optical flow detection and Bayesian forecast based on visual visible light communication is shown in Fig. 8. Firstly, initialize the priori probability in the first frame. Then calculate the optical flow for all pixels in the image to obtain the effective motion vector. After that, priori probability, conditional probability and posteriori probability of every pixel in the next frames can be calculated. Furthermore, in the experiment of shielded transmitter, shielding range is compared with a given threshold. If the range exceeds the threshold, the target LED in this image is considered to be incomplete, its coordinate would be forecasted based on posteriori probability. If the range does not exceed the threshold, the coordinate of the maximum motion vector is considered as the target LED position. Therefore, the terminal equipment can be located with strong robustness.

A video sequence was recorded with the industry camera introduced above to better explain the proposed algorithm and the experimental result. In the experiment, the trajectory of the smart car is controlled by a cell phone through Bluetooth. After adjusting the exposure time, there are only LEDs left in the images. Applying single-lamp positioning technology, the region of interest (ROI) shrinks to a small region so that we can position by the coordinate of only one LED. In other words, there is no need to get the coordinates of all four LEDs, the terminal equipment can be located so long as one of them is obtained, which decrease the computational cost.

3.2 Result and Analysis

3.2.1 Robustness Performance: In order to simplify the experiment, only single LED target is taken into consideration to validate the robustness performance of our algorithm in this part. In most cases, the LED target is fully rendered in the images, as shown in Fig. 9. In this situation, as the complete effective motion vector of the whole image can be obtained, the position of the LED target can be detected without forecasting. As can be seen from Fig. 9, the proposed algorithm can track and position the target LED accurately with small errors, which means that our algorithm possesses high positioning accuracy.

TABLE 1
Parameters of the Experimental Platform

Camera Specifications	
Model	MV-U300
Spectral Response Range/nm	400~1030
Resolution	800×600
Frame Rate/FPS	46
Dynamic Range/dB	>61
Signal-to-noise Ratio/dB	43
Pixel(H×V)	2048×1536
Pixel Size/μm²	3.2×3.2
Time of Exposure/ms	0.0556-683.8
Sensitivity	1.0V/lux-sec 550nm
Optical Filter	650nm Low Pass Optical Filter
Type of Shutter	Electronic Rolling Shutter
Acquisition Mode	Successive and Soft Trigger
Working Temperatures/°C	0-50
Support Multiple Visual Software	OpenCV, LabView
Support Multiple Systems	Vista, Win7, Win8, Win10
Experimental Platform Specifications	
Size (L×W×H)/ cm^3	190×100×190
LED Specifications	
Coordinates (x, y, z)/cm	LED1(100,45,190) LED2(100,145,190) LED3(0,145,190) LED4(0,45,190)
Diameter of each LED/mm	150
Power of each LED/W	6
The half-power angles of LED/deg($\varphi_{1/2}$)	60
Smart Car Specifications	
Single-chip	STC89C52RC
Weight/g	1200
Remote Control	Bluetooth, Wifi
Circuit Board Specifications	
Drive chip	DD311
Drive current/A	0.1
Drive voltage/V	28

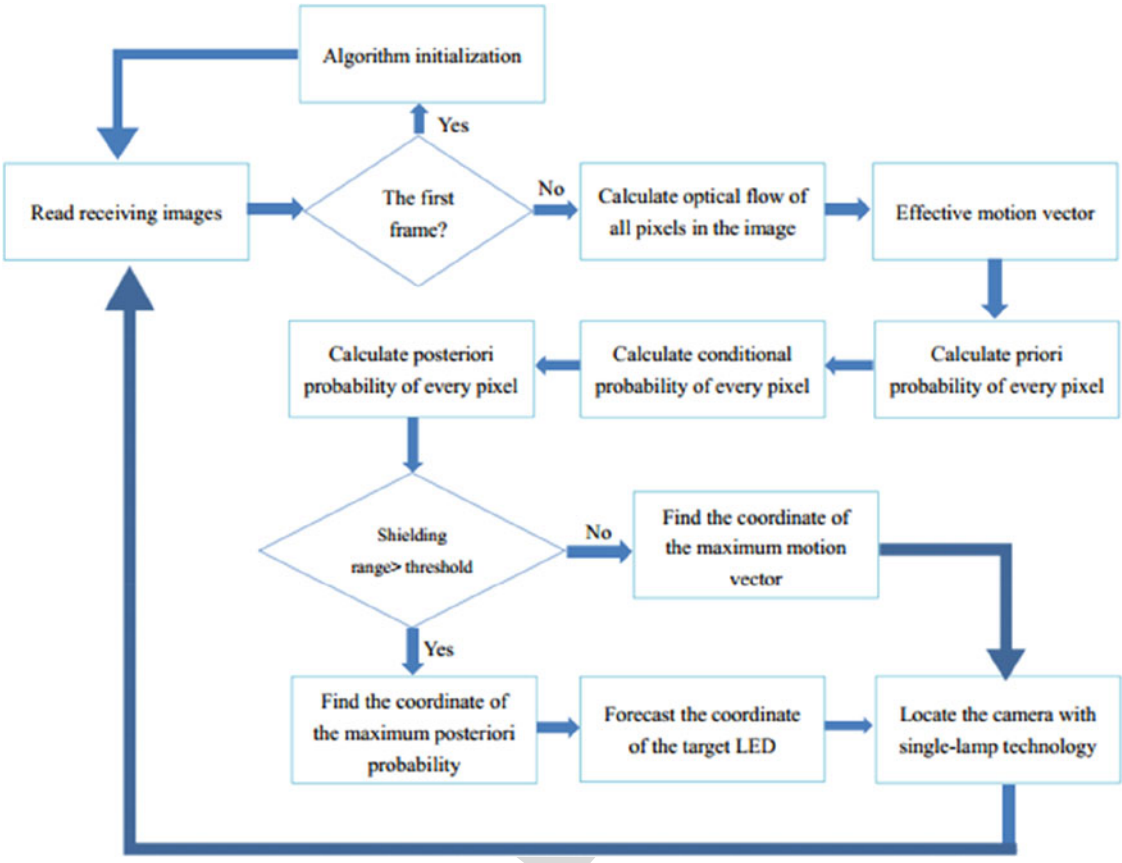

Fig. 8. Detailed procession of the proposed tracking and positioning algorithm.

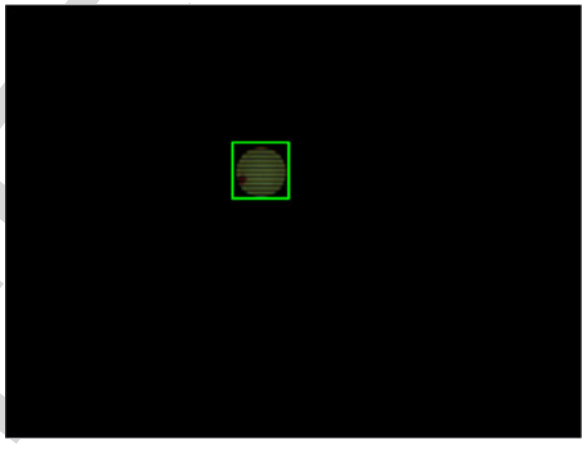

Fig. 9. Tracking performance when the LED is complete detected (without shielding).

Robustness is a vital index to judge the stability of the positioning system. As for VLP, shielding effect is a huge obstacle to robustness and even affects the success of positioning. There are several kinds of shielding effect classified by the shielded percentage, corresponding to the actual scenario. Almost equivalent to the broken LED, the situation of the LED shielded most part under the experimental condition is a special case of shielding effect, in which most valid data in the image

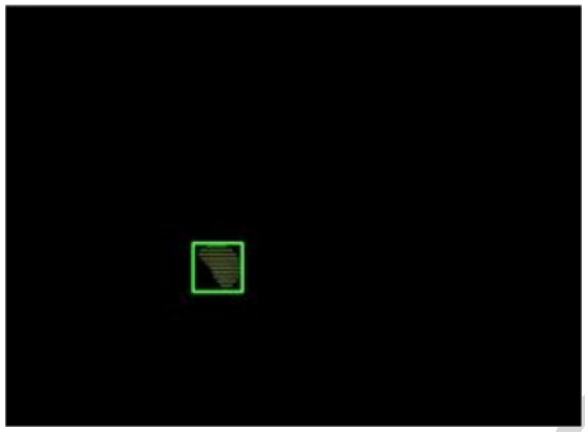

Fig. 10. Tracking performance when half of the LED is shielded.

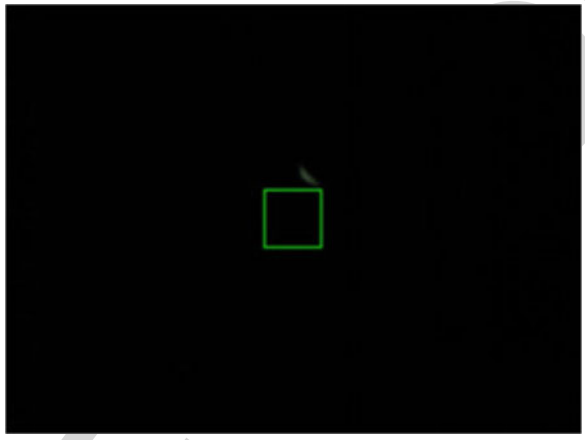

Fig. 11. Tracking performance when most part of the LED is shielded.

is lost. To test the robustness of the proposed positioning and tracking algorithm, we simulate the real situation and shield the target LED in different degrees. The results are shown as follows.

Firstly, as shown in Fig. 10, half of the target LED is shielded, the proposed algorithm can still detect and position it accurately. Although half of the target LED is lost in images, the remaining valid data can be obtained and naturally the position of camera can be calculated. The reason why it can achieve positioning under such adverse condition is that the proposed algorithm takes into account the optical flow of LED and information in the history and the calculated probability of the right LED coordinate still has a high accuracy. Furthermore, most part of the target LED is shielded. Because too much valid data is lost, the proposed algorithm locates the target LED with great error as shown in Fig. 11.

Moreover, shielding time is another vital influence factor for LED tracking. The target LED is shielded for a long period to test if our algorithm can locate the target LED accurately in the first frame after shielding. Fig. 12(a) is the first frame after shielding for a long period, which shows the algorithm can't locate the target LED accurately. But with the accumulation of valid data, the target LED can be located again, as is shown in Fig. 12(b). This indicates that the proposed algorithm can code with worse conditions even when the LED position is completely lost after the LED is shielded for a long period.

Last but not the least, a receiver operating characteristic curve (ROC) which is often used to judge the performance of Bayesian forecast algorithm, is plotted in Fig. 13 to show the robust-

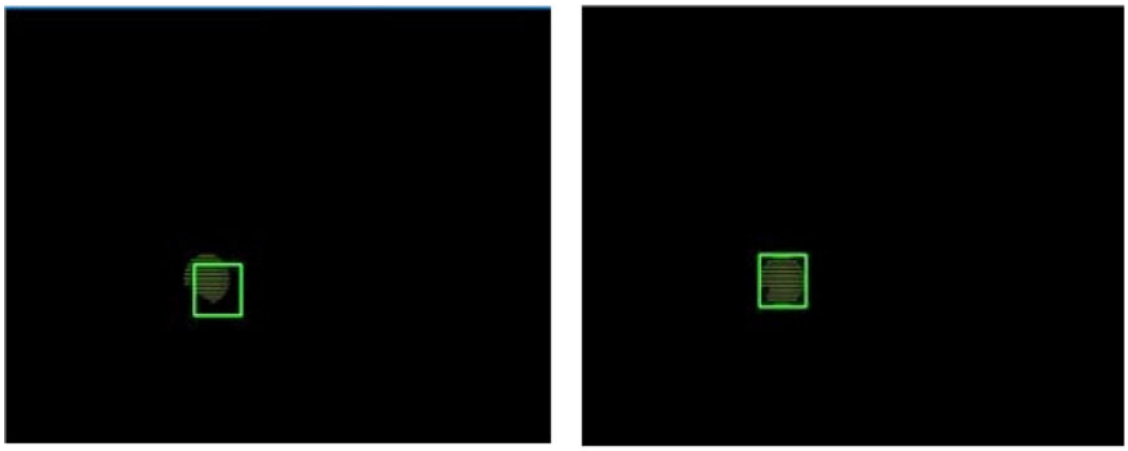

(a) (b)

Fig. 12. Tracking performance after the LED completely shielded for a long period; (a) the first frame after completely shielding for a long period; (b) the next few frames after completely shielding for a long period.

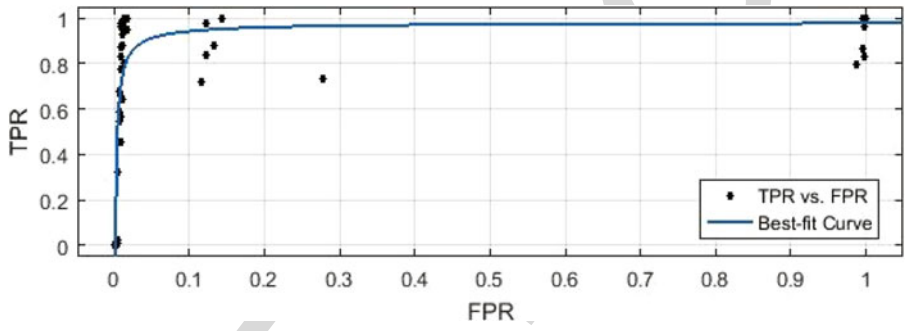

Fig. 13. The receiver operating characteristic curve (ROC) of the proposed positioning and tracking algorithm.

TABLE 2

The Contingency Table of the Bayesian Forecast Algorithm

		Forecast	
		1	0
Actual	1	True Positive (TP)	False Negative (FN)
	0	False Positive (FP)	True Negative (TN)

ness performance of the proposed tracking algorithm. Receiver operating characteristic curve, also known as sensitivity curve, is a comprehensive index that reflects the sensitivity and specificity of a continuous variable, using composition method to reveal the relationship between sensitivity and specificity. What's more, sensitivity values and specificity values are used as ordinate and abscissa respectively. In Bayesian forecast algorithm, the processing object is specified as a binary-problem: positive and negative (in the field of the proposed Bayesian forecast, the "positive" represents the forecast of the pixel is the LED, while the "negative" represents the forecast of the pixel is not the LED but the background). There are four cases in this binary-problem which can be seen in Table 2:

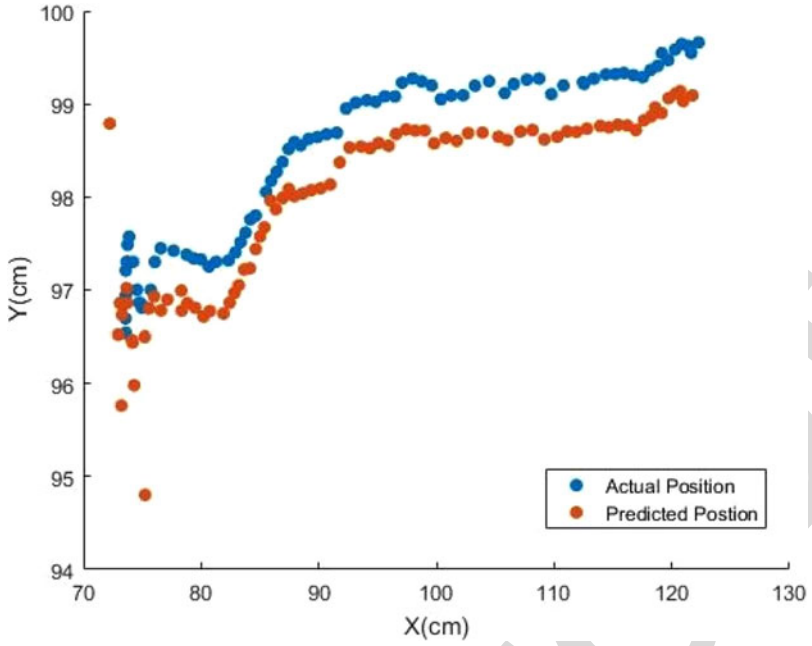

Fig. 14. The predicted positioning value and actual positioning value of the positioning terminal.

1) a positive object is predicted to be positive which is true positive (TP); 2) a negative object is predicted to be positive which is false positive (FP); 3) a negative object is predicted to be negative which is true negative (TN); 4) a positive object is predicted to be negative which is false negative (FN). Besides, Area Under Curve (AUC) of the ROC is between 0.5 and 1 (no practical meanings when less than 0.5). In general, through the value of the AUC, the performance of the proposed positioning and tracking algorithm can be measured as: (i) a lower accuracy when AUC is between 0.5 and 0.7; (ii) a certain accuracy when AUC is between 0.7 and 0.9; (iii) a good accuracy when AUC is between 0.9 and 1. Intuitively from the figure, the closer to the upper left corner, the better the performance of the algorithm. The greater area under curve the higher accuracy of the forecast.

The proposed algorithm is applied to a series of fifty images, and the true-positive rate (TPR) and false-positive rate (FPR) are calculated and represented as a dot in the Fig. 13. Then a series of scatter points are obtained. And we introduce a fitting curve to make the variation trend more visualized. Besides, the curve is obtained by using Trust Region algorithm, which is a quadratic approximate model and better than one-dimensional linear fitting. Therefore, it can be considered that the curve is the best fitting curve of the results of these dots. Since most of the results have an ideal performance and AUC is 0.954, it can be confirmed that the proposed Bayesian forecast algorithm has a good accuracy of prediction.

3.2.2 Accuracy Performance: The other main measure factor of the VLP is the positioning accuracy. Tracking error is defined as:

$$\mathrm{D} = \sqrt[2]{(x - x_r)^2 + (y - y_r)^2} \tag{42}$$

$$\text{error of } X \ \ (Y) = \left|\text{value}_{\text{predicted}} - \text{value}_{\text{actual}}\right| \tag{43}$$

where (x, y) represents the predicted position and (x_r, y_r) represent the actual position. In the recording video sequence, 80 successive frames without shielding are chosen to process. The result of positioning is shown in Fig. 14 where the blue dot represents the actual coordinate and the orange dot is the predicted coordinates for each sampling with the proposed algorithm. As can be seen from the result, the performance of the tracking positioning is well for most samples with small errors. In order to better illustrate the result and show the performance of the proposed algorithm,

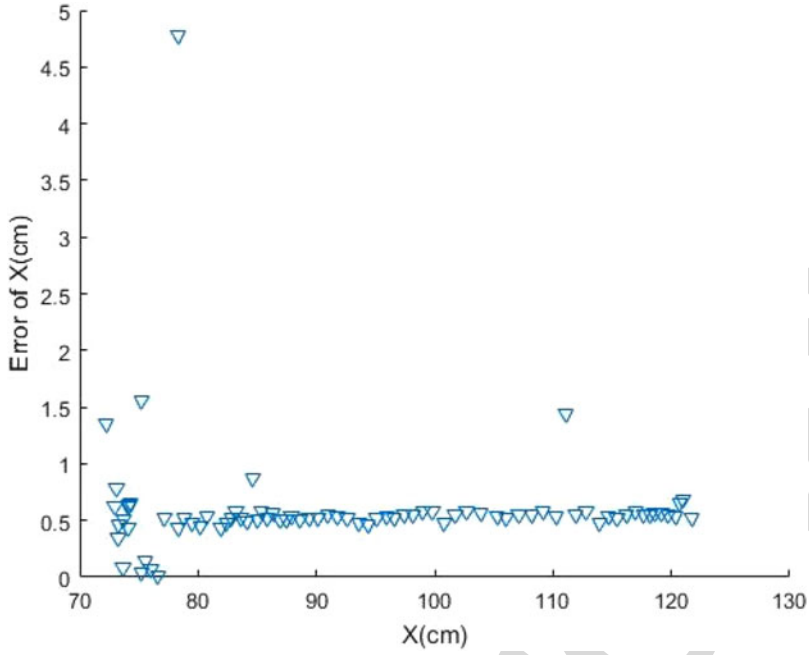

Fig. 15. Error of position value of x coordinates.

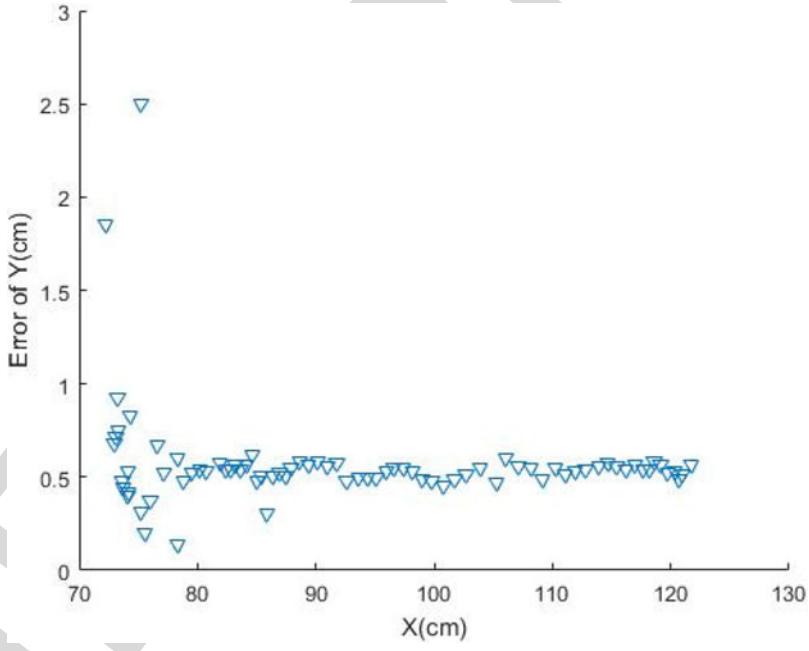

Fig. 16. Error of position value of y coordinates.

Figs. 15 and 16 show the error of x coordinates and y coordinates respectively. Average error of x coordinates is 0.55 cm and average error of y coordinates is 0.51 cm. But as can be seen from Figs. 15 and 16, there are several samples still have large error.

Fig. 17 shows that the tracking error D calculated by the definition of tracking error. As can be seen that, the maximum tracking error D is 4.78 cm, and average tracking error D is 0.86 cm. There are many reasons for the tracking error, such as image noise, which affects optical flow calculation

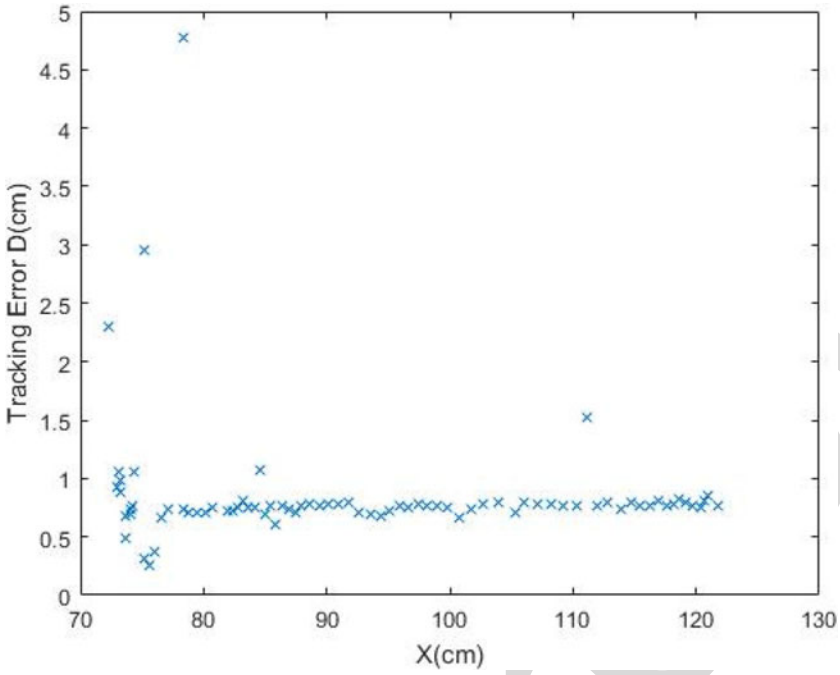

Fig. 17. The tracking error curve of the positioning terminal.

causing motion vector deviate from its actual value. Bayesian model has another inherent error because it's based on probability that means predicted position can have a great possibility fits with the actual position. However, there is still a possibility with a large deviation, causing tracking error always existing.

Cumulative distribution function (CDF) is the integral of the probability density function, which can describe the probability distribution of tracking error, error of x and y coordinates, shown in Fig. 18. As indicated by the curves, more than 90% tracking error D, the error of x, and the error of y is less than 0.99 cm, 0.67cm, and 0.67 cm, respectively. It means that if 90% is assumed as an acceptable service coverage rate, the proposed positioning and tracking algorithm will be able to deliver an accuracy of 0.99 cm.

3.2.3 Real-Time Performance: Running time of the program and complexity of the algorithm significantly affect real-time performance of tracking and positioning. Because it inevitably spends time to receive images and process data, when one coordinate is calculated, the terminal equipment has moved to the next coordinate already. In other words, positioning is always slower than the moving, especially when the terminal equipment moves fast. The proposed algorithm, using optical flow detection and Bayesian forecast, ensures the coordinate of the next moment can be calculated in advance under the premise of high accuracy.

Therefore, the maximum motion speed of the positioning terminal is an important index to evaluate the proposed algorithm. We hypothesis the target LED is tangent to the left edge of the image in frame N and is tangent to the right edge of the image in frame $N + 1$, shown in Fig. 19. The maximum motion speed of the positioning terminal v is defined as:

$$v = \frac{s}{t} \tag{44}$$

where s represents the distance of the terminal equipment moves between two successive frames, t represents the time of processing one frame. Based on the proportional relationship between images coordinate and world coordinate, relational expression is expressed as:

$$\frac{s}{r} = \frac{D}{d} \tag{45}$$

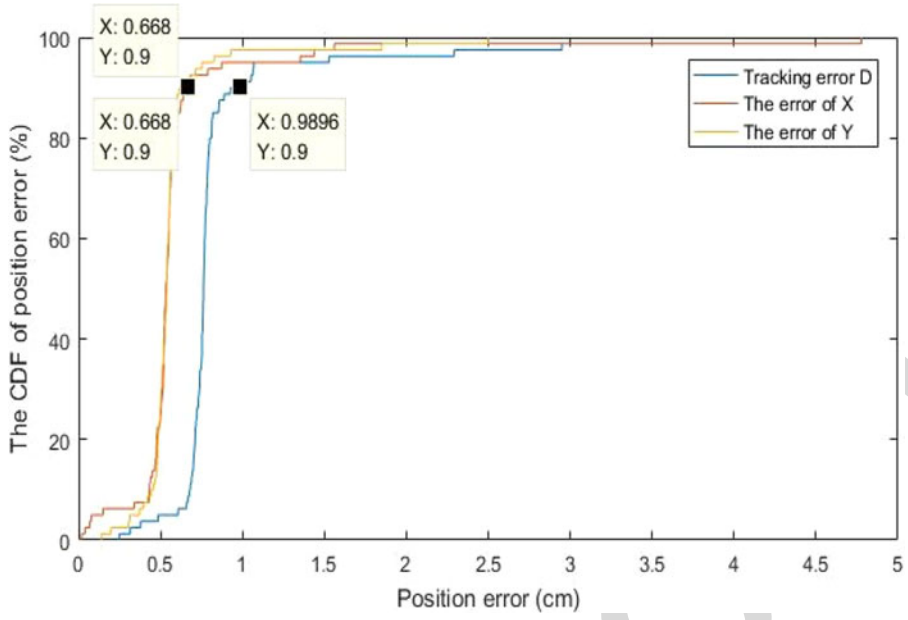

Fig. 18. The cumulative distribution function (CDF) of positioning error.

Fig. 19. The relative position of the LED in two successive frames.

where *r* represents pixel length of image, D represents the actual diameter of LED, and *d* represents the diameter of LED in images.

In our experimental environment, fifty successive frames of processing are chosen randomly to obtain the average running time *t* and learn that it is 0.162 s. According to Table 1, the real diameter D of LED is 150 mm. Besides, pixel length of images r is 800 (pixels) and the diameter of LED in images d is 55.54 (pixels), which is calculated with Hough transform. According to the definition of tracking speed, the maximum motion speed of the positioning terminal is 13.3362 m/s $\approx$ 48 km/h. which is far faster than that in [16], which can reach to 18 km/h. Besides, theoretically, the maximum tracking speed of our algorithm is even high enough for outdoor positioning, such as traffic system and tunnel. And this advantage of the proposed positioning and tracking algorithm opens the door to new possibility for outdoor dynamic positioning and tracking, in which the terminal is up to that speed or faster.

To further show the result of real-time performance, trajectory of the target LED can be drawn. There is no denying that only the algorithm has great real-time ability can the calculated trajectory coincide with the actual trajectory. Figs. 20(a) and (b) show the calculated trajectory with the proposed algorithm and actual trajectory, respectively. As can be seen from Fig. 20, the predicted

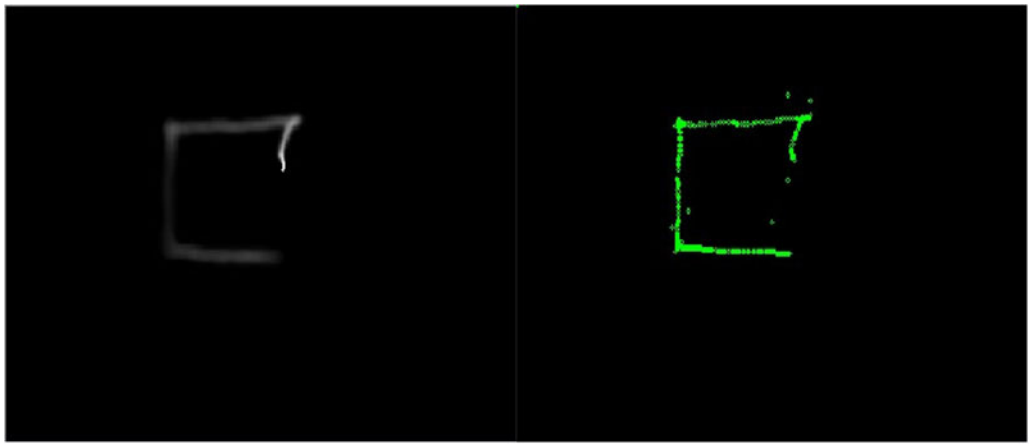

Fig. 20. The trajectory of the positioning terminal: (a) actual trajectory; (b) the output trajectory of the proposed algorithm.

trajectory forecasted by the proposed algorithm fits well with the actual trajectory, and only a few positions have large errors.

4. Conclusion

In this paper, we have developed and presented an algorithm for real-time indoor dynamic positioning and tracking based on VLP using image sensor, taking the advantage of optical flow and Bayesian forecast. These two methods solve the tricky problems in the field of VLP. Optical flow is used to overcome the difficulty of motion blur effect as it does not completely depend on pixel intensity. Besides, it can decrease the computational cost to ensure the good real-time ability of the proposed system. At the same time, Bayesian forecast is used to predict the position of positioning terminal when the light link between the LED and the positioning terminal is shielded or broken. It is important to highlight that the proposed algorithm achieves the real motion dynamic positioning and tracking in terms of positioning accuracy, real-time ability, terminal velocity and robustness, while most of the existing studies only achieve static fixed-point positioning or low-speed motion positioning. Finally, the proposed algorithm fuses the detection location information and the forecast location information by the WLS and adopts Kalman filtering to output the trajectory of the positioning terminal, which can adjust the weight of two information to fit different situations.

As for experiment, the proposed high-speed robust dynamic positioning and tracking method can realize a high positioning accuracy of 0.86 cm, and supports indoor positioning for terminal moving at a speed of up to 48 km/h. The proposed algorithm performs well in terms of positioning accuracy and real-time ability. Moreover, as for the robustness, the positioning terminal still can be located under the circumstance of shielded LED. All the results prove that the proposed algorithm have high positioning accuracy, good real-time ability, and strong robustness, which has a broad application prospect.

References

[1] T.-H. Do and M. Yoo, "An in-depth survey of visible light communication based positioning systems," *Sensors*, Basel, Switzerland, vol. 16, no. 5, May 12, 2016.
[2] Q. Peng, W. Guan, Y. Wu, Y. Cai, C. Xie, and P. Wang, "Three-dimensional high-precision indoor positioning strategy using Tabu search based on visible light communication," *Opt. Eng.*, vol. 57, no. 1, Jan. 2018.
[3] H. Chen, W. Guan, S. Li, and Y. Wu, "Indoor high precision three-dimensional positioning system based on visible light communication using modified genetic algorithm," *Opt. Commun.*, vol. 413, pp. 103–120, Apr. 15, 2018.

[4] W. Guan *et al.*, "A novel three-dimensional indoor positioning algorithm design based on visible light communication," *Opt. Commun.*, vol. 392, pp. 282–293, Jun. 1, 2017.
[5] Y. Cai, W. Guan, Y. Wu, C. Xie, Y. Chen, and L. Fang, "Indoor high precision three-dimensional positioning system based on visible light communication using particle swarm optimization," *IEEE Photon. J.*, vol. 9, no. 6, Nov. 11, 2017, Art. no. 7908120.
[6] W. Guan, Y. Wu, C. Xie, H. Chen, Y. Cai, and Y. Chen, "High-precision approach to localization scheme of visible light communication based on artificial neural networks and modified genetic algorithms," *Opt. Eng.*, vol. 56, no. 10, Oct. 1, 2017.
[7] W. Wuan *et al.*, "High precision three-dimensional iterative indoor localization algorithm using code division multiple access modulation based on visible light communication," *Opt. Eng.*, vol. 55, no. 10, Oct. 1, 2016.
[8] M. Yasir, S.-W. Ho, and B. N. Vellambi, "Indoor position tracking using multiple optical receivers," *J. Lightw. Technol.*, vol. 34, no. 4, pp. 1166–1176, Feb. 15, 2016.
[9] W. Guan, Y. Wu, C. Xie, L. Fang, X. Liu, and Y. Chen, "Performance analysis and enhancement for visible light communication using CMOS sensors," *Opt. Commun.*, vol. 410, pp. 531–545, Mar. 1, 2018.
[10] C. Xie, W. Guan, Y. Wu, L. Fang, and Y. Cai, "The LED-ID detection and recognition method based on visible light positioning using proximity method," *IEEE Photon. J.*, vol. 10, no. 2, Apr. 2018, Art. no. 7902116.
[11] Y. Wang, Y. Gong, and Z. Shi, "Research on the collinear equation model of visual positioning based on visible light communication," in *Proc. MATEC Web Conf. Int. Conf. Eng. Technol. Appl.*, vol. 22, Jul. 9, 2015.
[12] R. Zhang, W.-D. Zhong, Q. Kian, and S. Zhang, "A single LED positioning system based on circle projection," *IEEE Photon. J.*, vol. 9, no. 4, Aug. 2017, Art. no. 7905209.
[13] J.-Y. Kim, S.-H. Yang, Y.-H. Son, and S.-K. Han, "High-resolution indoor positioning using light emitting diode visible light and camera image sensor," *IET Optoelectron.*, vol. 10, no. 5, pp. 184–192, Oct. 1, 2016.
[14] Md. S. Hossen, Y. Park, and K.-D. Kim, "Performance improvement of indoor positioning using light-emitting diodes and an image sensor for light-emitting diode communication," *Opt. Eng.*, vol. 54, no. 3, Mar. 1, 2015.
[15] M. Alsalami Farah, "Game theory Minimax filter design for indoor positioning and tracking system using visible light communications," in *Proc. 6th Int. Conf. Inf. Commun. Manage.*, Dec. 14, 2016, pp. 197–200.
[16] J. Fang *et al.*, "High-speed indoor navigation system based on visible light and mobile phone," *IEEE Photon. J.*, vol. 9, no. 2, Apr. 2017, Art. no. 8200711.
[17] A. Luttman, E. Bollt, and J. Holloway, "An optical flow approach to analyzing species density dynamics and transport," *J. Comput. Math.*, vol. 30, pp. 249–261, 2012.
[18] T. Senst, V. Eiselein, and T. Sikora, "In Ii-Ik – a real-time implementation for sparse optical flow," in *Proc. Int. Conf. Image Anal. Recognit.*, 2010, pp. 240–249.
[19] J. Farrell, *Aided Navigation: GPS With High Rate Sensors*. New York, NY, USA: McGraw-Hill, Inc., 2008.
[20] D. F. Zheng, K. Y. Cui, B. Bai, G. Chen, and J. A. Farrell, "Indoor localization based on leds," in *Proc. IEEE Int. Conf. Control*, 2011, pp. 573–578.
[21] D. B. Reid, "An algorithm for tracking multiple targets," *IEEE Trans. Autom. Control*, vol. AC-24, no. 6, pp. 843–854, Dec. 1979.

Queries

Q1. Author: Please verify that the funding information is correct.

Q2. Author: Please provide the page range in Refs. [1], [2], [6], [7], [11], and [14].